

# Supramolecular electrolytes with multiple hydrogen bonds for solid state dye-sensitized solar cells

La Sun Jeon<sup>a</sup>, Sun-Young Kim<sup>a</sup>, Su Jin Kim<sup>a</sup>, Yong-Gun Lee<sup>b</sup>, Moon-Sung Kang<sup>c</sup>, Yong Soo Kang<sup>a,\*</sup>

<sup>a</sup> Center for Next Generation Dye-Sensitized Solar Cells, WCU Program Department of Energy Engineering, Hanyang University, Seongdong-gu, Seoul 133-179, South Korea

<sup>b</sup> School of Chemical and Biological Engineering, Seoul National University, San 56-1, Sillim-dong, Gwanak-gu, Seoul 151-742, South Korea

<sup>c</sup> Corporate R&D Center, Samsung SDI, 428-5 Gongse-dong, Yongin-si, Gyeonggi-do, South Korea

## ARTICLE INFO

### Article history:

Received 20 December 2009

Received in revised form 19 February 2010

Accepted 29 March 2010

Available online 4 April 2010

### Keywords:

Supramolecular polymer

Hydrogen bonding

Dye-sensitized solar cells

## ABSTRACT

Oligomeric supramolecules with double- (2H-P), triple- (3H-P) and quadruple H-bonding sites (4H-P) at their both chain ends of PEG ( $M_w=2000$ ) are successfully utilized to increase energy conversion efficiency for solid state dye-sensitized solar cells. The improved energy conversion efficiency is due mostly to the deeper penetration of the liquid oligomeric supramolecular electrolytes into the nanopores of the  $\text{TiO}_2$  layer, followed by *in situ* self-polymerization via multiple H-bonds and the improved ionic conductivity. Among the three solid state dye-sensitized solar cells, the 2H-P and 3H-P electrolytes shows better photovoltaic performances than the 4H-P electrolyte. The difference in the performance is mostly attributable to the fact that the 2H-P and 3H-P electrolytes have a slower electron recombination rate and a faster ionic diffusion coefficient, compared to the 4H-P electrolyte. Therefore, the characters of the liquid and the solid states of the supramolecules may have been able to be successfully utilized to increase the energy conversion efficiency over 4% for solid state dye-sensitized solar cells.

© 2010 Elsevier B.V. All rights reserved.

## 1. Introduction

Considerable attention has been focused on dye-sensitized solar cells (DSSCs) because of their advantages such as high energy conversion efficiency and low production cost [1,2]. DSSCs are categorized into solid or liquid state DSSCs depending on the state of the electrolytes. Solid state DSSCs employing polymer electrolytes have also been becoming more attractive because of their intrinsic advantages such as long-term durability and a cost-effective fabrication process [3,4]. However, their energy conversion efficiency is very low, compared to the 11% of liquid type DSSCs [5]. This difference is mostly because of the low ionic conductivity of the solid polymer electrolyte and the poor interfacial contact between the dye molecules and the electrolyte. For example, a polymer electrolyte with a coil size of 50–100 nm would have shallow penetration into the nanopores of 10–20 nm in mesoporous  $\text{TiO}_2$  layer, resulting in poor interfacial contact and consequently poor conversion efficiency [6–9].

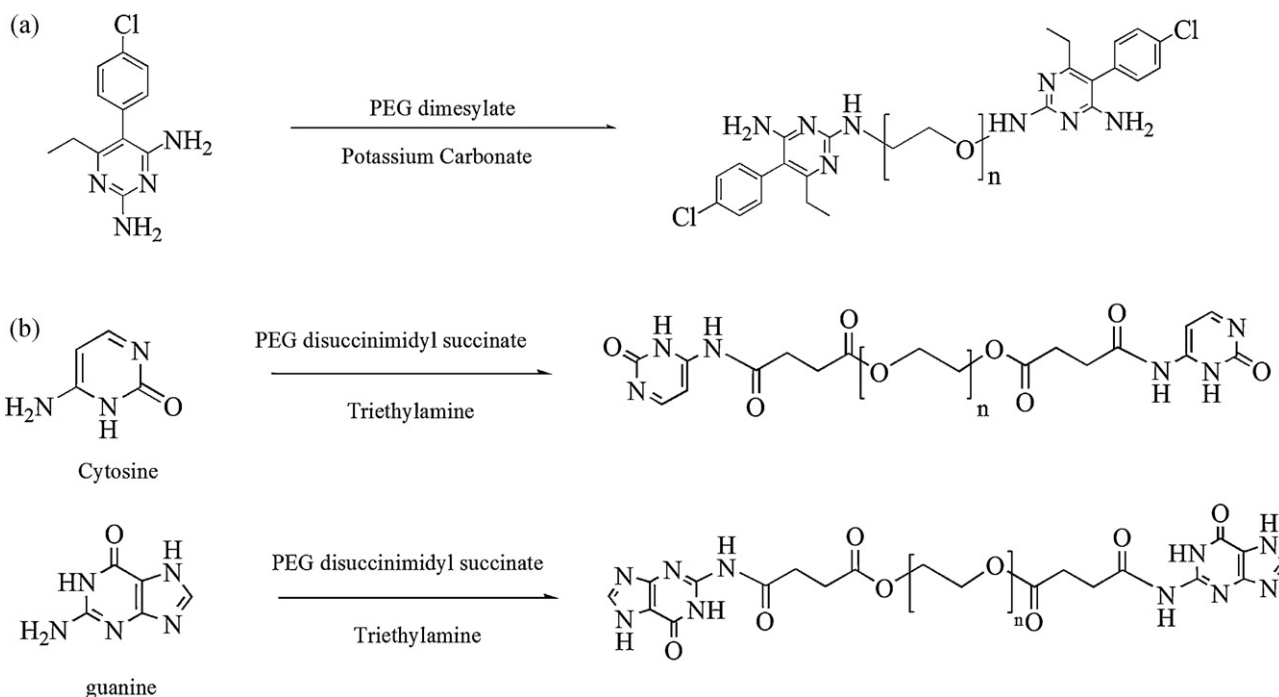
Recently, several research groups have investigated to increase the overall conversion efficiency of solid and quasi-solid state DSSCs [10–13]. A vacuum pore-filling method was used to

increase the penetration depth of polymer electrolytes for solid state dye-sensitized solar cells [10a]. Polymer-based electrolytes comprising a copolymer poly(ethylene oxide-co-epichlorohydrin) with  $\gamma$ -butyrolactone was successfully optimized to achieve the high ionic conductivity ( $\sim 1 \text{ mS cm}^{-1}$ ) [10b]. The straight pores in  $\text{Al}_2\text{O}_3$ /ionic liquid modified with amylose was utilized as ionic paths [11]. Spiro-OMeTAD (2,2',7,7'-tetrakis(N,N-dimethoxyphenylene)-9,9'-spirofluorene) was used as a hole transporting material to make fully solid state DSSCs [12]. Using photochemically polymerized poly(3,4-ethylenedioxythiophene) (PEDOT) as a hole transporting material, infiltration of PEDOT into nanopores of the  $\text{TiO}_2$  layer was significantly enhanced and thus the interfacial property between the dye molecules and the hole-conducting material was significantly improved [13].

Previously we were able to improve the efficiency of solid state DSSCs by 3–4% using an “Oligomer Approach” [18]. An oligomer has a typical molecular weight of several thousand with a radius gyration of less than 3 nm. It is in liquid state at room temperature, while a common polymer with a molecular weight of 1 million has a radius of gyration of  $\sim 50$  nm. It has been observed that the average diameter of the nanopores in the  $\text{TiO}_2$  layer is  $\sim 15$  nm [14]. Therefore, deeper penetration of the oligomers into the nanopores of the  $\text{TiO}_2$  layer is expected to enlarge the interfacial contact between the electrolyte and the dyes. The oligomers were subsequently solidified by ether blending with high molecular weight polymers [14], incorporating nanoparticles such as silica nanoparticles [15] or forming quadruple H-bonds [16,17]. Low molecular components

\* Corresponding author at: Center for Next Generation Dye-Sensitized Solar Cells, WCU Program Department of Energy Engineering, Hanyang University, Seongdong-gu, Seoul 133-179, South Korea. Tel.: +82 2 2220 2336; fax: +82 2 2296 2969.

E-mail address: [kangys@hanyang.ac.kr](mailto:kangys@hanyang.ac.kr) (Y.S. Kang).



**Scheme 1.** Synthesis of the supramolecular polymer electrolytes: (a) double hydrogen bonding polymer (2H-P) and (b) triple hydrogen bonding polymer (3H-P).

and oligomers have thus been polymerized by three different ways in order to make the electrolytes the solid state [18].

Oligomeric supramolecules containing multiple hydrogen bonding sites at both chain ends of poly(ethylene glycol) (PEG) oligomer have been utilized here to improve the ionic conductivity as well as overall conversion efficiency by enlarging the interfacial contact area between the solid state electrolyte and the dyes. Previously, supramolecular polymer electrolytes with quadruple H-bonding sites were successfully employed with an energy conversion efficiency of 3.34% at  $100 \text{ mW cm}^{-2}$  for solid state DSSCs [17,18].

Here we synthesized and utilized new oligomeric supramolecules with double and triple H-bonding sites at both chain ends of PEG with a molecular weight of 2000, resulting in improved energy conversion efficiency for solid state DSSCs. Thus, the performances of the three cells were compared and characterized in terms of the charge transport behavior including the electrons and ions, in particular the electron recombination and the ionic diffusion coefficient.

## 2. Experimental

### 2.1. Material synthesis

Oligomeric supramolecules containing double hydrogen bonds were synthesized as shown in Scheme 1(a). Poly(ethylene glycol) dimesylate ( $M_w = 2000 \text{ g mol}^{-1}$ ) was purchased from Fluka and pyrimethamine, glutaric acid and potassium carbonate from Aldrich. Pyrimethamine (0.435 g, 1.75 mmol) was dissolved in 15 mL of THF, and potassium carbonate (0.242 g, 1.75 mmol) was added to the solution. Then poly(ethylene glycol) dimesylate (0.5 g, 0.25 mmol) was dropped slowly into the solution. The resulting mixture was stirred for 24 h at  $70^\circ\text{C}$  under nitrogen atmosphere. After the reaction was complete, the reaction mixture was added to ACN (25 mL) and filtered. This process was repeated several times. The filtrate was evaporated in a vacuum oven until dried.  $^1\text{H NMR}$  (300 MHz,  $\text{CDCl}_3$ ):  $\delta$  [ppm] = 7.5 (d, H; CH) 7.2 (d, H; CH) 6.9 (s, 2H;  $\text{NH}_2$ ), 4.4 (m, H; NH), 3.6 (m, 2H;  $\text{CH}_2$ ), 3.5–3.7

(m, 2H;  $\text{CH}_2$ ), 2.5 (m, 2H;  $\text{CH}_2$ ), 1.2 (m, 3H;  $\text{CH}_3$ ), 0.89 (m, 3H;  $\text{CH}_3$ ).

Glutaric acid (0.42 g, 3.17 mmol) dissolved in 20 mL ACN was added to the polymer solution and the mixture was stirred overnight at room temperature. The solution was then dried in an oven at  $30^\circ\text{C}$ , and the product was washed by ACN. After being dried, 2H-P was obtained.

Two oligomeric supramolecules containing guanine (G-PEG-G) and cytosine (C-PEG-C) at both chain ends of the PEG were synthesized according to Scheme 1(b) [19,20]. Poly(ethylene glycol) disuccinimidyl succinate ( $M_w = 2000$ , PEG-SS) was purchased from Sunbio (Korea), guanine and triethylamine from Aldrich and cytosine from TCI. Guanine (0.264 g, 1.75 mmol) was dissolved in 15 mL of THF, and then triethylamine (TEA) (0.176 g, 1.75 mmol) was added to the solution followed by PEG disuccinimidyl succinate (PEG-SS) (0.5 g, 0.25 mmol), which was dropped slowly into the solution. The mixture was stirred at  $80^\circ\text{C}$  for 24 h under a nitrogen atmosphere, and the mixture was then filtered after adding 20 mL of ACN. The solution was dried in a vacuum oven for 1 day (until dried).  $^1\text{H NMR}$  (300 MHz,  $\text{CDCl}_3$ ): 8.0 (m, H; NH) 4.2 (m, 2H;  $\text{CH}_2$ ), 3.4–3.7 (m, 2H;  $\text{CH}_2$ ), 2.9 (m, 2H;  $\text{CH}_2$ ), 2.8 (s, H; NH), 2.7 (m, 2H;  $\text{CH}_2$ ), 2.6 (s, H; CH), 2.0 (s, H; NH), 1.4 (m, 2H;  $\text{CH}_2$ ). C-PEG-C was synthesized with the same method for G-PEG-G from cytosine rather than guanine.  $^1\text{H NMR}$  (300 MHz,  $\text{CDCl}_3$ ):  $\delta$  [ppm] = 12.2 (m, H; NH), 8.3 (m, H; NH), 4.2 (m, 2H;  $\text{CH}_2$ ), 3.5–3.7 (m, 2H;  $\text{CH}_2$ ), 2.9 (m, H; CH), 2.8 (s, 2H;  $\text{CH}_2$ ), 2.7 (m, H; CH), 2.0 (s, H; NH).

Two G-PEG-G and C-PEG-C were mixed for 24 hrs in ACN (25 mL) at  $30^\circ\text{C}$  to make hydrogen bonds between guanine and cytosine. The solution was then dried at  $40^\circ\text{C}$  in atmospheric condition for several days.

### 2.2. Cell fabrication and performances

Dye-sensitized solar cells were fabricated using a previously published method [21]. Nanoporous  $\text{TiO}_2$  films (thickness =  $12 \mu\text{m}$ ) were prepared on transparent conductive oxide (TCO) (Nippon Sheet Glass,  $\text{SnO}_2/\text{F}$ ,  $8 \text{ ohm/sq}$ ) from  $\text{TiO}_2$  nanoparticles (STI) by annealing at  $450^\circ\text{C}$  in air for 30 min. Dyes were absorbed by

dipping the film into a solution containing 0.3 mM Ru dye (Bu4N)-[Ru(Hdcbpy)<sub>2</sub>(NCS)<sub>2</sub>] (known as N719, Solaronix). And then the electrolyte was induced onto a working electrode. Solar cells were made by placing a Pt-coated glass on the TiO<sub>2</sub> film. The typical cell area was approximately 0.16 cm<sup>2</sup>, separated by a thickness of 25 μm. The standard electrolytes consisted of 1.113 M 3-propyl-1-methylimidazolium iodide (PMII) and 10 wt% of I<sub>2</sub> with respect to PMII. The *J*–*V* curves were determined using a Solar Simulator with delay time and NPLC of 100 ms and 1 PLC, respectively, under an illumination of 100 mW cm<sup>−2</sup> by a 50–500 WXe lamp (Thermo Oriol Instruments, USA). The cell temperature during illumination was increased from ambient (~20 °C) to 30–40 °C. The performance was measured after 10 min of illumination because the curves were stabilized normally after 5 min of illumination. As a reference, a simple liquid type DSSC of an electrolyte of 0.6 M PMII, 0.1 M LiI, 0.05 M I<sub>2</sub>, 0.5 M *tert*-butylpyridine, 0.05 M guanidine thiocyanate in ACN with the active area of 0.16 cm<sup>2</sup> and TiO<sub>2</sub> layer thickness of 12 μm was prepared, resulting in *J*<sub>sc</sub>, *V*<sub>oc</sub> and *η* of 14.1 mA cm<sup>−2</sup>, 0.75 V and 7.87, respectively.

### 2.3. Ionic diffusion coefficient

The electrolyte solutions consisting of a supramolecular polymer electrolyte with multiple (double, triple and quadruple) H-bonding sites were sandwiched between two platinum coated FTO electrodes with 25 μm thick Surlyn spacer. The active area for electrolyte packaging was 0.4 cm × 0.4 cm. A potentiostat system (AUTOLAB) was used for the steady-state voltammogram [22].

### 2.4. Electron lifetime

The electron lifetime of the TiO<sub>2</sub> layer was measured by stepped light-induced transient measurements [23]. A diode laser (Coherent, LabLaser, λ 635 nm) was employed for the photovoltage transients. The absorption coefficient of the N719 dye at this wavelength is negligible thus to have nearly uniform electron generation along the thickness (6 μm) of the DSSCs. Irradiation to the whole area of the DSSCs, the laser beam was expanded by a lens, and an aperture was placed in front of the solar cell. The transients were induced by the stepwise change of the laser intensity controlled by a function generator. A set of ND filters was used to change the laser intensity. Photovoltage transients were monitored by a digital storage oscilloscope through a current amplifier (SR570, Stanford Research Systems) and a differential amplifier (5307, NF Electronic Instruments) with a gain of 20 times was used to monitor the few millivolts of decay of the photovoltage.

### 2.5. Impedance spectra

The impedance of the supramolecular polymer electrolytes was measured with an impedance analyzer (IM6, Zahner) connected to a potentiostat in the dark. The electrochemical impedance spectra were recorded over a frequency range of 50 mHz to 1 MHz. The applied voltage was 10 mV and was set at *V*<sub>oc</sub> of the cells [24].

## 3. Results and discussion

### 3.1. Formation of supramolecular polymers via multiple H-bonds

Oligomeric poly(ethylene glycol) (PEG) with a Mw of 2000 was chemically modified to become supramolecules with multiple H-bonding sites at both chain ends. The molecular weight of 2000 for the oligomers with the small coil size of about 3 nm was utilized to enhance the penetration of the electrolyte into nanopores (average diameter ~15 nm) of TiO<sub>2</sub> layer [18]. The chemical structures of the oligomeric supramolecules and the corresponding supramolecular

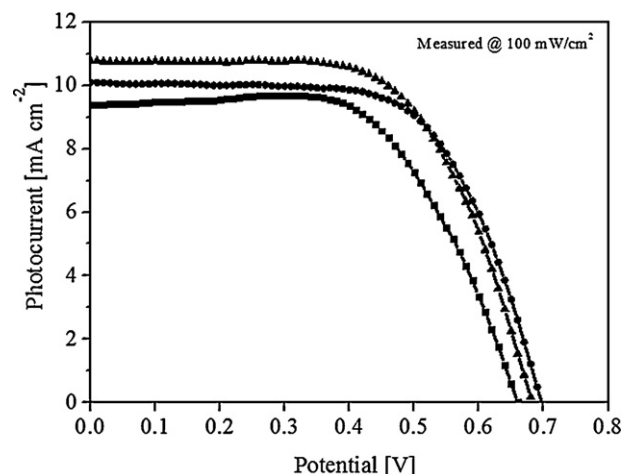


**Fig. 1.** *J*–*V* curves of the DSSCs using supramolecular polymer electrolytes: double H-bonding polymer (2H-P, triangle), triple H-bonding polymer (3H-P, circle), and quadruple H-bonding polymer (4H-P, square).

polymers with double (2H-P), triple (3H-P) and quadruple (4H-P) H-bonds are depicted in Scheme 2. The supramolecules in solution have a coil shape of less than 3 nm in size and become supramolecular polymers by forming multiple H-bonds after evaporation of the solvent [17]. Thus, the properties of both the liquid and solid states can be utilized to improve the interfacial contact between the electrolyte and the dyes and to provide the solid state electrolyte with increased ionic conductivity.

### 3.2. Photovoltaic performances

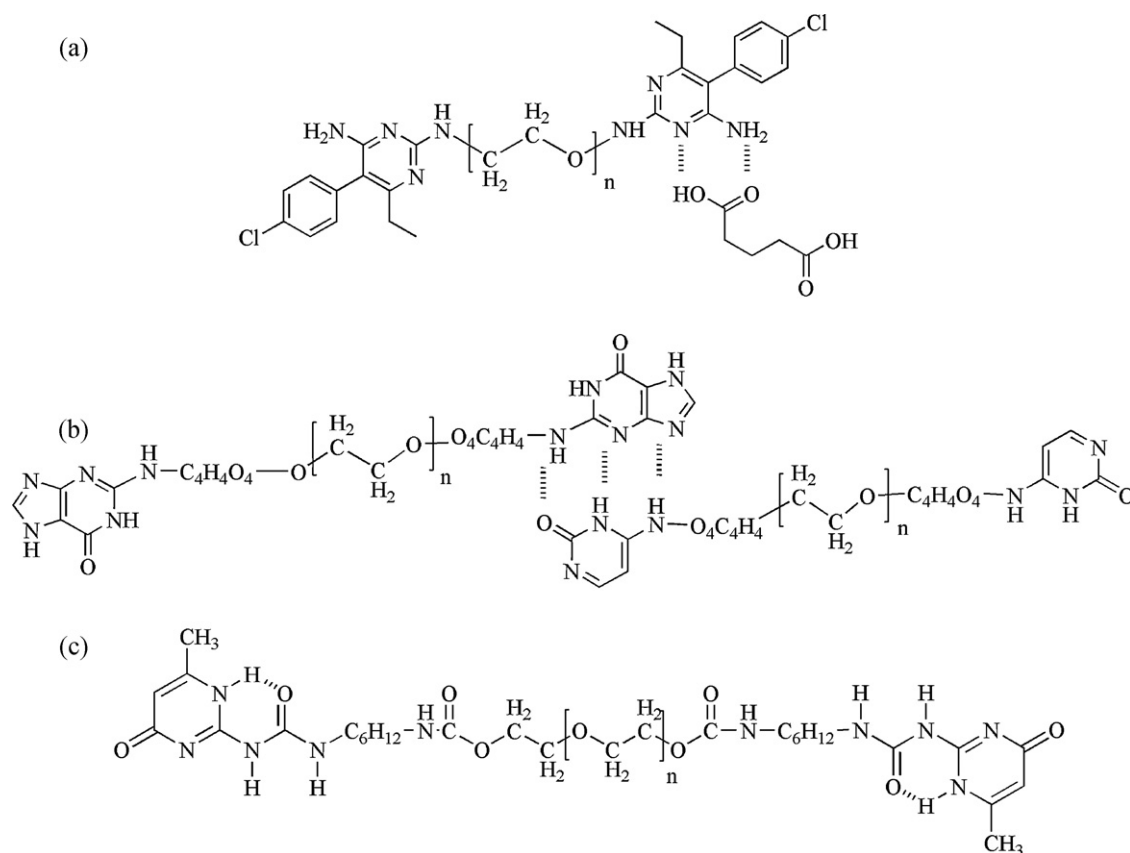
The *J*–*V* curves of the DSSCs employing supramolecular polymer electrolytes were obtained as shown in Fig. 1. The electrolyte compositions for both the 2H-P, 3H-P and 4H-P electrolytes were fixed at a molar ratio of 20:1 (1.113 M) for the ethylene oxide unit of PEG: PMII and the iodine concentration of 10 wt% with respect to PMII. The energy conversion efficiency, *η*, for the 3H-P cell was 4.53% at 1 sun condition with a short-circuit current density of *J*<sub>sc</sub> = 10.10 mA cm<sup>−2</sup>, an open circuit voltage of *V*<sub>oc</sub> = 0.69 V and a fill factor of *FF* = 0.64. For that of the 2H-P cell it was 4.63% with *J*<sub>sc</sub> = 10.78 mA cm<sup>−2</sup>, *V*<sub>oc</sub> = 0.68 V and *FF* = 0.63. The performances for both the 2H-P and 3H-P cells were improved to a large extent, compared to 3.78% for the 4H-P [17]. All results are summarized in Table 1. The improved energy conversion efficiency by utilizing supramolecular polymer electrolytes, compared to the efficiency of 1.6% by polymer electrolytes [3] was primarily due to the better interfacial contact associated with the deeper penetration of the oligomeric supramolecules into the nanopores of the TiO<sub>2</sub> layer and the increased ionic conductivity (~1 × 10<sup>−4</sup> S cm<sup>−1</sup>) to some extent [18]. Among the three cells utilizing 2H-P, 3H-P and 4H-P electrolytes, the 2H-P cell showed the highest efficiency. In the following sections, the three cells were characterized to understand the difference in the cell performance in terms of the electron recombination and the ionic conductivity.

**Table 1**

Photovoltaic performance of DSSCs using supramolecular polymer electrolytes.<sup>a</sup>

Matrix	<i>J</i> <sub>sc</sub> [mA cm <sup>−2</sup> ]	<i>V</i> <sub>oc</sub> [V]	<i>FF</i>	Eff. [%]
2H-P	10.78	0.67	0.63	4.63
3H-P	10.10	0.70	0.64	4.53
4H-P	9.4	0.65	0.62	3.78

<sup>a</sup> Composition of electrolytes: Mole ratio of EO unit of matrix/PMII = 20/1 (1.113 M) and I<sub>2</sub> with 10 wt% of PMII.



**Scheme 2.** Structures of the supramolecular polymer electrolytes: (a) double hydrogen bonding polymer (2H-P), (b) triple hydrogen bonding polymer (3H-P) and (c) quadruple hydrogen bonding polymer (4H-P) [17].

### 3.3. Electron recombination

When electrons injected into the  $\text{TiO}_2$  layer flow rapidly toward the electrode, the energy conversion efficiency will be high. However, when the electron transport rate is low, some electrons react with  $\text{I}_3^-$ , resulting in a loss of electrons and consequently the loss of energy conversion efficiency, which is termed electron recombination. Electron recombination can be characterized by the electron lifetime in the  $\text{TiO}_2$  layer and the dark current. If the electron recombination is fast, the electrons on the  $\text{TiO}_2$  layer do not have enough of a lifetime to flow into the photoanode, but may have more chance to recombine with  $\text{I}_3^-$  instead. Thus, the electron lifetime as a measure of the rate of electron recombination was obtained by stepped light-induced transient measurements of the photocurrent and the voltages (SLIM-PCV) [23,25–27]. Fig. 2 shows the lifetime of the electrons in the nanocrystalline  $\text{TiO}_2$  film as a function of their short-circuit current density. As expected, the electron lifetime decreased with  $J_{sc}$ . At low short-circuit current densities, the electron lifetime of the 4H-P electrolyte was much longer than the other two. As the short-circuit current density increased, the electron lifetimes for 2H-P and 3H-P decreased slowly, while that of 4H-P decreased much more steeply. The steeper decrease in the lifetimes for 4H-P seems to be owing to the accumulation of  $\text{I}_3^-$  ions near the  $\text{TiO}_2$  layer induced by the slow mass transport in the electrolyte. The polymeric chains of 4H-P were more rigid than the other two because of the more H-bonds between chains, resulting in the stronger dependency of light intensity or short-circuit current density on the electron life time. From these results, it can be estimated that the electron lifetimes of 4H-P are much shorter than those of 2H-P and 3H-P at the practical short-circuit current density range (i.e.  $\sim 10 \text{ mA cm}^{-2}$ ), suggesting that it was the fastest electron recombination among the three different electrolytes. The results

of the electron lifetime are also consistent with those of  $V_{oc}$  shown in Table 1 and Fig. 1.

Impedance spectra as Cole–Cole plots were obtained for the three cells under dark conditions and are shown in Fig. 3. The plots show two semicircles, representing the charge transfer resistance at the counter electrode in the high frequency range, and the interfacial impedance between the electrode and the dyes in the mid-frequency range [24,23]. The impedance in the mid-frequency range is associated with the electron recombination [28]. The impedance data again suggests that the 4H-P electrolyte showed a smaller impedance than the other two. Under dark con-

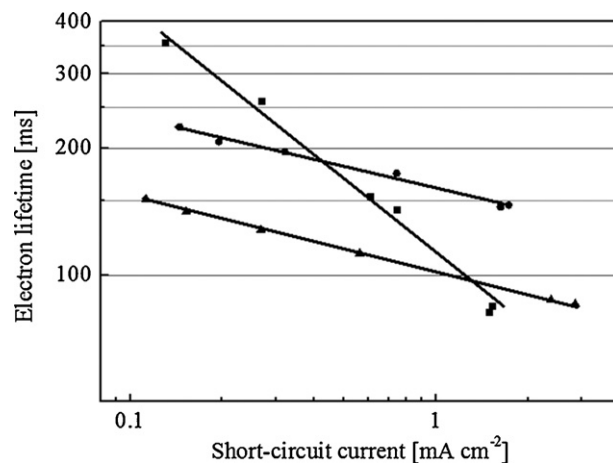


**Fig. 2.** Electron lifetime for supramolecular polymer electrolytes as a function of short-circuit density: double H-bonding polymer (2H-P, triangle), triple H-bonding polymer (3H-P, circle) and a quadruple H-bonding polymer (4H-P, square).



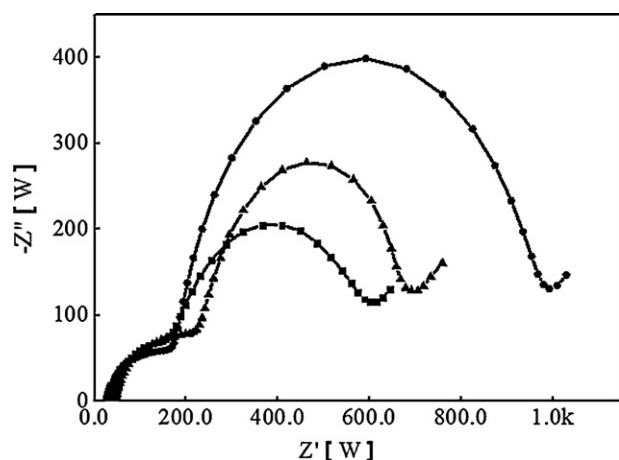


**Fig. 3.** Impedance spectra for solid state DSSCs using supramolecular polymer electrolytes: double H-bonding polymer (2H-P, triangle), triple H-bonding polymer (3H-P, circle) and a quadruple H-bonding polymer (4H-P, square).

**Table 2**

Diffusion coefficients of  $I^-$  in DSSCs using a supramolecular polymer electrolyte.<sup>a</sup>

Matrix	$j$ -limited ( $\text{mA cm}^{-2}$ )	$D$ ( $\text{cm}^2 \text{s}^{-1}$ )
2H-P	1.33	$1.69 \times 10^{-7}$
3H-P	1.12	$1.43 \times 10^{-7}$
4H-P	0.73	$0.93 \times 10^{-7}$

<sup>a</sup> Composition of electrolytes: Mole ratio of EO unit of matrix/PMII = 20/1 (1.113 M) and  $I_2$  with 10 wt% of PMII.

ditions, the value of impedance for the supramolecular polymer electrolyte was decreased in the order of 3H-P, 2H-P and 4H-P. These results also suggest that the 4H-P electrolyte showed the fastest recombination rate among the three cells. The impedance results are consistent with those of the electron lifetime behavior. It was thus concluded that the slow electron recombination on the  $\text{TiO}_2$  layer, as confirmed by the measurement of the electron lifetime and the dark impedance, may contribute to some extent to the improved energy conversion efficiency for 2H-P and 3H-P.

### 3.4. Ion transport in electrolyte

The low energy conversion efficiency for the solid state DSSCs has been mostly blamed for the low ionic conductivity of the electrolyte component. It should be noted that the ionic conductivity is a product of the ionic concentration and its mobility, which can be characterized by the diffusion coefficient [29]. The diffusion coefficients were obtained by measuring the limiting current density with steady-state voltammogram as follows [30–32]:

$$I_{ss} = 4nFDC,$$

where  $I_{ss}$  is the limiting current density,  $n$  is the electron number,  $F$  is the Faraday constant,  $D$  is the diffusion coefficient of  $I^-$  or  $I_3^-$ , and  $C$  is the bulk concentration of the electroactive species. The results of the steady-state voltammograms for the three cells are summarized in Table 2. The diffusion coefficient of  $I^-$  was decreased in the order of the 2H-P, 3H-P and 4H-P electrolytes. Note that the ionic diffusion coefficient tends to decrease with the number of hydrogen bonds. In other words, the 4H-P showed the lowest diffusion coefficient. This may be primarily because the more number of H-bonding sites between the oligomeric chains, the more rigid the polymer chain becomes. These results suggest that the chain strength and mobility of the supramolecular polymers containing multiple H-bonds can also be controlled by the number of H-bonds.

## 4. Conclusions

Oligomeric supramolecules were successfully utilized to increase the energy conversion efficiency of solid state dye-sensitized solar cells up to 4.6% at 1 sun condition. The 2H-P and 3H-P electrolytes showed better performance than the 4H-P electrolyte. The improved performances for solid state dye-sensitized solar cells utilizing the 2H-P and 3H-P electrolytes were likely due to the slower electron recombination rates and the faster ionic conductivity of the 2H-P and 3H-P electrolytes compared to the 4H-P electrolyte. Finally, it was concluded that the utilization of oligomeric supramolecules was an effective avenue to improve the energy conversion efficiency of solid state dye-sensitized solar cells.

## Acknowledgements

This research was supported by Nano R&D program (2008-03599), ERC program (2009-0063369) through National Research Foundation of Korea funded by the Ministry of Education, Science and Technology and the MKE(The Ministry of Knowledge Economy), Korea, under the ITRC(Information Technology Research Center) support program supervised by the NIPA(National IT Industry Promotion Agency)(NIPA-2009-C1090-0804-0013).

## References

- [1] B. O'Regan, M. Grätzel, A low-cost, high-efficiency solar cell based on dye-sensitized colloidal  $\text{TiO}_2$  films, *Nature* 353 (1991) 737–740.
- [2] K. Hara, T. Sato, R. Katoh, A. Furube, Y. Ohga, A. Shinpo, S. Suga, K. Sayama, H. Sugihara, H. Arakawa, Molecular design of coumarin dyes for efficient dye-sensitized solar cells, *J. Phys. Chem. B* 107 (2003) 597–606.
- [3] A.F. Nogueira, J.R. Durrant, M.A. De Paoli, Dye-sensitized nanocrystalline solar cells employing a polymer electrolyte, *Adv. Mater.* 13 (2001) 826–830.
- [4] A.F. Nogueira, C. Longo, M.A. De Paoli, Polymers in dye sensitized solar cells: overview and perspectives, *Coord. Chem. Rev.* 164 (2004) 1455–1468.
- [5] S. Ferrere, B.A. Gregg, Large increases in photocurrents and solar conversion efficiencies by UV illumination of dye sensitized solar cells, *J. Phys. Chem. B* 105 (2001) 7602–7605.
- [6] W. Kubo, S. Kambe, S. Nakade, T. Kitamura, K. Hanabusa, Y. Wada, S. Yanagida, Photocurrent-determining processes in quasi-solid-state dye-sensitized solar cells using ionic gel electrolytes, *J. Phys. Chem. B* 107 (2003) 4374–4381.
- [7] B. Li, L. Wang, B. Kang, P. Wang, Y. Qiu, Review of recent progress in solid-state dye-sensitized solar cells, *Sol. Energy Mater. Sol. Cells* 90 (2006) 549–573.
- [8] V.C. Nogueira, C. Longo, M.A. De Paoli, M.A. Soto-Oviedo, A.F. Nogueira, Solid-state dye-sensitized solar cell: improved performance and stability using a plasticized polymer electrolyte, *J. Photochem. Photobiol. A: Chem.* 181 (2006) 226–232.
- [9] T. Kato, A. Okazaki, S. Hayase, Latent gel electrolyte precursors for quasi-solid dye sensitized solar cells, *Chem. Commun.* (2005) 363–365.
- [10] (a) H. Han, U. Bach, Y.-B. Cheng, R.A. Caruso, Increased nanopore filling: effect on monolithic all-solid-state dye-sensitized solar cells, *Appl. Phys. Lett.* 90 (2007), 213510-1–1213510-3; (b) J.N. de Freitas, A.S. Gonçalves, M.A. De Paoli, J.R. Durrant, A.F. Nogueira, EDLC performance of carbide-derived carbons in aprotic and acidic electrolytes, *Electrochim. Acta* 53 (2008) 7166–7172.
- [11] T. Kogo, S. Hayase, T. Kaiho, M. Taguchi, Quasi-solid dye sensitized solar cells having straight ion paths, *J. Electrochem. Soc.* 155 (2008) K166–K169.
- [12] G. Boschloo, T. Marinado, K. Nonomura, T. Edvinsson, A.G. Agrios, D.P. Hagberg, L. Sun, M. Quintana, C.S. Karthikeyan, M. Thelakkat, A. Hagfeldt, A comparative study of a polyene-diphenylamine dye and  $\text{Ru}(\text{dcbpy})_2(2\text{NCS})_2$  in electrolyte-based and solid-state dye-sensitized solar cells, *Thin Solid Films* 516 (2008) 7214–7217.
- [13] (a) Y. Kim, Y.-E. Sung, J.-B. Xia, M. Lira-Cantu, N. Masaki, S. Yanagida, Solid-state dye-sensitized  $\text{TiO}_2$  solar cells using poly(3,4-ethylenedioxythiophene) as substitutes of iodine/iodide electrolytes and noble metal catalysts on FTO counter electrodes, *J. Photochem. Photobiol. A: Chem.* 193 (2008) 77–80; (b) J. Xia, N. Masaki, M. Lira-Cantu, Y. Kim, K. Jiang, S. Yanagida, Effect of doping anions' structures on poly(3,4-ethylenedioxythiophene) as hole conductors in solid-state dye-sensitized solar cells, *J. Phys. Chem. C* 112 (2008) 11569–11574.
- [14] M.S. Kang, J.H. Kim, Y.J. Kim, J. Won, N.-G. Park, Y.S. Kang, Dye-sensitized solar cells based on composite solid polymer electrolytes, *Chem. Commun.* (2005) 889–891.
- [15] J.H. Kim, M.S. Kang, Y.J. Kim, J. Won, N.-G. Park, Y.S. Kang, Dye-sensitized nanocrystalline solar cells based on composite polymer electrolytes containing fumed silica nanoparticles, *Chem. Commun.* (2004) 1662–1663.
- [16] B.J.B. Folmer, E.W. Meijer, Supramolecular polymer materials: chain extension of telechelic polymers using a reactive hydrogen-bonding synthon, *Adv. Mater.* 12 (2000) 874–878.

- [17] Y.J. Kim, J.H. Kim, M.S. Kang, M.J. Lee, J. Won, J.C. Lee, Y.S. Kang, Supramolecular electrolytes for use in highly efficient dye-sensitized solar cells, *Adv. Mater.* 16 (2004) 1753–1757.
- [18] M.S. Kang, J.H. Kim, J. Won, Y.S. Kang, Supramolecular electrolytes for use in highly efficient dye-sensitized solar cells, *J. Phys. Chem. C* 111 (2007) 5222–5228.
- [19] M.S. Kang, K.-S. Ahn, J.-W. Lee, Quasi-solid-state dye-sensitized solar cells employing ternary component polymer-gel electrolytes, *J. Power Sources* 180 (2008) 896–901.
- [20] L. Han, N. Koide, Y. Chiba, T. Mitate, Modeling of an equivalent circuit for dye-sensitized solar cells, *Appl. Phys. Lett.* 84 (2004) 2433–2435.
- [21] H. Usui, H. Matsui, N. Tanabe, S. Yanagida, Improved dye-sensitized solar cells using ionic nanocomposite gel electrolytes, *J. Photochem. Photobiol. A: Chem.* 164 (2004) 97–101.
- [22] B.M. Quinn, Z. Ding, F. Moulton, A.J. Bard, Novel electrochemical studies of ionic liquids, *Langmuir* 18 (2002) 1734–1742.
- [23] P. Wang, S.M. Zakeeruddin, P. Comte, I. Exnar, M. Grätzel, Gelation of ionic liquid-based electrolytes with silica nanoparticles for quasi-solid-state dye-sensitized solar cells, *J. Am. Chem. Soc.* 125 (2003) 1166.
- [24] N. Fukuri, N. Masaki, T. Kitamura, Y. Wada, S. Yanagida, Electron transport analysis for improvement of solid-state dye-sensitized solar cells using poly(3,4-ethylenedioxythiophene) as hole conductors, *J. Phys. Chem. B* 110 (2006) 25251–25258.
- [25] R. Kawano, M. Watanabe, Equilibrium potentials and charge transport of an  $I^-/I_3^-$  redox couple in an ionic liquid, *Chem. Commun.* (2003) 330–331.
- [26] J.K. Tessmar, A.G. Mikos, A. Göpferich, Amine-reactive biodegradable diblock copolymers, *Biomacromolecules* 3 (2002) 194–200.
- [27] J. Röstlin, A.-L. Smeds, E. Åkerblom, B-domain deleted recombinant coagulation factor VIII modified with monomethoxy polyethylene glycol, *Bioconjug. Chem.* 11 (2000) 387–396.
- [28] H. Nishide, S. Iwasa, Y.-J. Pu, T. Suga, K. Nakahara, M. Satoh, Organic radical battery: nitroxide polymers as a cathode-active material, *Electrochim. Acta* 50 (2004) 827–831.
- [29] L. Brunsveld, R.P. Sijbesma, Supramolecular polymers, *Chem. Rev.* 101 (2001) 4071–4098.
- [30] S. Nakade, T. Kanzaki, T. Kitamura, Y. Wada, S. Yanagida, Stepped light-induced transient measurements of photocurrent and voltage in dye-sensitized solar cells: application for highly viscous electrolyte systems, *Langmuir* 21 (2005) 10803–10807.
- [31] Z. Zhang, P. Chen, T.N. Murakami, S.M. Zakeeruddin, M. Grätzel, The 2,2,6,6-tetramethyl-1-piperidinyloxy radical: an efficient, iodine-free redox mediator for dye-sensitized solar cells, *Adv. Funct. Mater.* 18 (2008) 341–346.
- [32] S. Nakade, T. Kanzaki, S. Kambe, Y. Wada, S. Yanagida, Investigation of cation-induced degradation of dye-sensitized solar cells for a new strategy to long-term stability, *Langmuir* 21 (2005) 11414–11417.